dc electrical conductivity of D-T gas

W. G. Wolfer and C. L. Bisson
Sandia National Laboratories, Livermore, California 94550

P. C. Souers and R. T. Tsugawa
Department of Chemistry and Materials Science, Lawrence Livermore National Laboratory, Livermore, California 94550

(Received 5 April 1989; revised manuscript received 27 November 1989)

The space charge and the electrical current in a weakly ionized radioactive gas is theoretically evaluated. The results are compared with experimental data for a deuterium gas at room temperature containing 0.1 mol % of tritium. The dc electrical conductivity has been measured for gas densities from 0.1 to 10 mol/l and applied voltages over the range 0.1 to 400 V. The resulting current density increases with increasing gas density and the decreases at higher densities. The theoretical results show that the charge-density profiles in the gas as well as the space-charge potential change dramatically with the applied voltage. Varying the electronic recombination coefficients until theoretical predictions agree with the measured results provides a means to determine them. From this comparison it is found that the three-body recombination coefficients is 6.2×10^{-26} cm^6 s^{-1}, whereas the two-body recombination coefficient is indeterminate and of little influence on the quality of the fit as long as its value is below 10^{-5} cm^3 s^{-1}.

I. INTRODUCTION

The radioactive decay of tritium offers a convenient way to produce in a precise and uniform manner electron-ion pairs in gases or even in condensed phases which readily dissolve hydrogen. Since the decay product is ^{3}He, no chemically reactive species are introduced than hydrogen. It is then possible to study with this technique various aspects of interest to radiochemistry, such as electron mobility and electron-ion recombination in dense gases and in liquids.

In the present paper we are specifically addressing two issues: the effect of space charge on the current-voltage characteristics of a weakly ionized gas and the magnitude of the electron-ion recombination coefficient in a dense hydrogen gas. The first issue takes us back in history to the pioneering work of Thompson[1,2] on the conduction of electricity through gases and to the attempts by him and his contemporaries to theoretically derive the current-voltage law. The second issue deals with a current research topic, namely, the electronic collisional-dissociative recombination of molecular ions in dense gases. These two aspects are closely related in the present study, because our ability to accurately compute the current-voltage characteristic also enables us to determine the value of the recombination coefficient required to bring theory and experiments into close agreement.

II. THEORETICAL FORMULATION

The experimental and theoretical configuration of interest for the present study is a gas gap of width L confined between two parallel metal plates to which an external electrical potential V can be applied. At a sufficient distance from the plate edges the electric field is uniform and perpendicular to the plates. The analysis as well as the plate area from which current is drawn in the actual experiment will be restricted to this one-dimensional region. In this region $0\le x\le L$, the concentrations of ions and electrons, $p(x)$ and $n(x)$ satisfy the two diffusion equations

$$\frac{\partial p}{\partial t}+\nabla j_p=G-\alpha pn \ , \tag{1}$$

$$\frac{\partial n}{\partial t}+\nabla j_n=G-\alpha np \ , \tag{2}$$

where G is the generation rate per unit volume of ion-electron pairs, α is a recombination coefficient to be specified later on, and

$$j_p=-D_p\nabla p+pD_p\nabla U \ , \tag{3}$$

$$j_n=-D_n\nabla n-nD_n\nabla U \ , \tag{4}$$

are the fluxes of ions and electrons. Here, D_p and D_n are the diffusion coefficients for ion and electrons, respectively, and

$$U=e\Phi/kT-eVx/LkT \ , \tag{5}$$

with e the elementary charge, k the Boltzmann constant, and T the absolute temperature. The electrostatic potential in the equation above is divided into a space-charge potential Φ and the applied potential Vx/L. The former is determined from the Poisson equation

$$\nabla^2\Phi=-4\pi e(p-n) \tag{6}$$

and the boundary conditions that Φ vanish on the metal plates.

We can also assume that the charges are neutralized once they come in contact with the metal plates, so that the boundary conditions for the charge concentrations are $n(0)=n(L)=p(L)=0$

The solution of Eqs. (1), (2), and (6) has been considered by numerous researchers in the fields of gaseous electronics and plasma physics as well as in various branches of semiconductor technology. In attempts by Thompson[1,2] and by Boucher,[3] the diffusion terms in Eqs. (3) and (4) were neglected, and recombination within the space-charge regions were treated in an approximate manner. When retaining the diffusion terms, numerical approaches were employed, e.g., by Allis and Rose,[4] Gusinov and Gerber,[5] and an asymptotic analysis was developed by Cohen and Kruskal.[6] Extensive numerical studies are routinely carried out nowadays in the context of semiconductor device modeling,[7] and we shall therefore not elaborate on the numerical method used in this study to solve the above equations. However, we would like to discuss one important aspect in the numerical determination of the current-voltage relationship. Once the charge-density distributions $p(x)$ and $n(x)$ have been numerically obtained, it is in principle possible to evaluate their gradients at the metal plates and use Eqs. (3) and (4) to find the current $I=j_p(0)-j_n(0)$. Because of the steep concentration gradients near the metal plates, however, the numerical accuracy that can be obtained in determining the difference of two large gradients was found to be insufficient. As a result, an explicit expression for the current I had to be derived as follows. For the one-dimensional and stationary case of interest here, Eqs. (1) and (2) can be formally integrated twice, and the two integration constants can be determined from the boundary conditions. The net current is then found to be given by

$$I=j_p(x)-j_n(x) = \frac{\int_0^L e^{-U(x')}Q(x')dx'}{\int_0^L e^{-U(x')}dx'} - \frac{\int_0^L e^{U(x')}Q(x')dx'}{\int_0^L e^{U(x')}dx'} , \quad (7)$$

where the cumulative source function is defined as

$$Q(x)=\int_0^x [G-\alpha p(x')n(x')]dx' . \quad (8)$$

The formula (7) displays several important facts. First, the stationary current is independent of the position x, as it must be. Second, all regions in space need to be considered for providing to the current, including those regions where the recombination rate is equal to the generation rate and the cumulative source function exhibits a plateau region. Third, the function $I(V)$ cannot simply be represented as a power law. Fourth, when recombination and space-charge effects are negligible, then $Q(x)=G(x)$, and Eq. (7) can be evaluated to give the saturation current $I_{\max}=GL$, which is the charge-generation rate in the gas volume swept out by the unit area of collecting surface.

III. APPLICATION TO D-T MIXTURES

A. Charge generation

The average kinetic energy carried off by the electron emitted in the radioactive decay of tritium nucleus[8] is 5.69 keV. This energy is expended in ionization, excitation, dissociation, and elastic collisions with the molecules of the surrounding gas. Careful measurements have been carried out by Combacher[9] to determine the energy expended by energetic electrons to produce ion-electron pairs in hydrogen and deuterium gases. This energy was found to be 34.6 eV for electron energies greater than about 100 eV. Accordingly, every β decay of a tritium nucleus produces on average about 165 ion-electron pairs. With the decay rate constant for tritium[8] of $\lambda=1.782\times10^{-9}$ s^{-1}, the charge-generation rate is given by $G_0=165\lambda f(2N)$, where N is the density of molecules per cm^3 in the gas mixture and f is the tritium enrichment factor. This form of the charge-generation rate requires some modification near the walls of the gas container. The electron emitted in the radioactive decay has a finite range κ^{-1} over which the ionization events are distributed. All energetic electrons emitted by tritium atoms at distances from the wall less than this range and in directions towards the wall will dissipate some of their energy in the wall material. The charge generation is therefore expected to drop off from its maximum value in the interior of the gas gap to half this value at the wall. This decline near the wall is expected to be nearly exponential, and the following equation for the generation rate expresses this behavior:

$$G(x)=330\lambda fN[1-\exp(-\kappa L)\cosh(\kappa|2x-L|)] . \quad (9)$$

The absorption of tritium β particles in hydrogen has been measured by Dorfman,[10] and his results yield an extinction coefficient given by $\kappa/N=7.36\times10^{-20}$ cm^2.

B. Diffusion and mobilities

Other parameters required for the numerical analysis are the diffusion coefficients and the mobilities of the charge-carrying species. The mobilities are in fact the appropriate parameters that control the drift terms in Eqs. (3) and (4), and the replacement of the mobility μ with the relationship $\mu=De/kT$ is strictly valid only when the charged particles either gain less energy between collisions than the thermal energy or when their momentum-transfer cross section is independent of their velocity. The measured ratio of D_n/μ_n for electrons in deuterium[11] varies by about a factor of 4 over the range of values for V/LN encountered in the present experiment. This variation was found to be of little significance in the analysis, as the ion mobility is the more prominent limiting factor for the steady-state current. Therefore, an average value of 0.09 nm^2 was selected for the momentum-transfer cross section[11] to determine the electron mobility and diffusion coefficient given (in cm^2 s^{-1}) by

$$D_n=2.7\times10^{-20}[(N/\sqrt{T})(1+5.69\times10^{-21}N/\sqrt{T})]^{-1} . \quad (10)$$

This coefficient also includes the effects of multiple scattering of the electrons at high gas densities according to the theory of Braglia and Dallacasa.[12]

The primary ionic species produced by the β particles are D^+ and D_2^+ as well as their equivalents when D is replaced by tritium. However, these ions quickly convert

to D_3^+, which in turn may bind another D_2 molecule to become D_5^+ at the pressures encountered in this study. Larger ion clusters are much less stable and need not be considered here. Assuming that these two dominant ion species are in thermodynamic equilibrium with each other and with the gaseous molecules, the effective ion mobility is given by

$$\mu_p=(\mu_3+\mu_5 K_{53}N)/(1+K_{53}N) . \quad (11)$$

Here, μ_3 is the mobility of D_3^+ which has been experimentally determined by Miller *et al.*[3] to be 8.0 $cm^2 s^{-1} V^{-1}$ at 0 ° C and 1 atm gas pressure. The mobility of the heavier ion can be estimated by using the reduced mass for the ion-molecule collision as a scaling factor. Accordingly, μ_5 is found to be equal to 7.34 $cm^2 s^{-1} V^{-1}$. Expressed as a function of gas density, these mobilities are

$$\mu_3=2.15\times10^{12}/N \quad (12)$$

and

$$\mu_5=1.97\times10^{12}/N . \quad (13)$$

The equilibrium constant K_{53} has been determined by Hiraoka and Kebarle[14] and more recently by Elford.[15] Both measurements are in good agreement and give

$$K_{53}=3.72\times10^{-20}\exp(1141.4/T)\ cm^3 . \quad (14)$$

In addition to the variability predicted by Eq. (11) for the primary ion mobility as a function of gas density and temperature, small amounts of other molecules in the D-T mixture may also influence the effective ion mobility. In the experiments discussed below, such molecules as O_2, N_2, CO_2, and D_2O are present in the gas at a few parts per million level. With the exception of O_2, these trace molecules have a higher proton affinity than D_2. In addition, the concentration of primary ions is only on the order of 10 parts per billion, as the numerical results below will show. As a result, deuteron transfer reactions will take place when the primary ions encounter these trace molecules, and the dominant molecular ions in the gas are those which form with these trace molecules, e.g., D_3O^+. Its mobility is estimated to be 9.2 $cm^2 s^{-1} V^{-1}$ based on the measured mobility[16] for H_3O^+ in H_2 of 12.6 $cm^2 s^{-1} V^{-1}$. The mobilities of D_3^+, D_3O^+, and other trace molecular ions differ therefore only by about 15%, and this difference was found to affect the computed current through the gas cell by less than 2%. As a result, Eq. (11) can and will be used for most of the numerical results given below.

C. Recombination

For the high neutral gas densities encountered in the present experimental situation, the collisional-dissociative recombination process[17] is dominant. This process may be viewed as two-step mechanism, with electron capture into a Rydberg level representing the first step followed by the decay of the excited state through dissociation. The capture into a stable Rydberg level may be accompanied by electron-energy loss to adjacent molecules, in which case three-body collisions become important. Accordingly, we may write for the total recombination coefficient

$$\alpha=\alpha_2+\alpha_3 N . \quad (15)$$

For the two-body dissociative recombination process, electron capture either results in an electronic state of the intermediate molecule that is repulsive, or if it is an attractive Rydberg state, this state crosses another repulsive state which is reached by collisional deexcitation. The magnitude of this recombination process is strongly dependent on the vibrational level in the attractive Rydberg state. The recombination of H_3^+, for example, has been measured in a microwave afterglow discharge,[18] in inclined beams,[19] in merged beams, [20–23] and in ion traps.[24] In all these experimental techniques, vibrationally excited H_3^+ ions are produced and retained until recombination. These "hot" ions possess a dissociative recombination coefficient α_2 which is of order 10^{-6} $cm^3 s^{-1}$ at 300 K. In contrast, in flowing afterglow discharges,[25,26] thermally equilibrated H_3^+ ions can be produced, and the dissociative recombination was measured to be at or below the detection limit of 2×10^{-8} $cm^3 s^{-1}$. This implies a negligible recombination coefficient α_2 for "cold" H_3^+ ions. In dense gases, the most likely reaction for these ions is then to form H_5^+, and it is this molecular ion that will subsequently recombine. The corresponding dissociative recombination coefficient α_2 has been measured[18,27] and the results can be represented by the empirical expression

$$\alpha_2(H_5^+)=4.5\times10^{-6}(100/T)^{1/2}\ cm^3 s^{-1} . \quad (16)$$

Since the vibrational state of the H_5^+ ions was not known, however, it is questionable whether this recombination coefficient can be applied to cold ions. The dissociative recombination of other molecular ions such as H_3O^+ in H_2 has not been measured up to now.

The theoretical model[17] for the three-body recombination coefficient α_3 of molecular ions with internal degrees of freedom does not render itself to a closed-form solution, but the numerical results can be approximated by the empirical expression

$$\alpha_3=A(300/T)^n , \quad (17)$$

with two fitting parameters A and n. The exponent n may vary from 0.4 to 2.5 depending on the gas, its density, and the coupling strength between the Rydberg and the dissociative states. The magnitude of A is found to be approximately an order of magnitude larger than for the three-body recombination of H^+ in its parent gas H_2. For this case, Bates, Malaviya, and Young[28] were able to predict α_3, with A being about 10^{-26} $cm^6 s^{-1}$ at 300 K.

Given the lack of more precise theoretical models or better experimental data, we treat the two recombination coefficients in Eq. (15) as adjustable parameters within the confines of the above discussions, and match our theoretical predictions to the experimental results.

IV. EXPERIMENT

The schematic diagram of the electrical cell is shown in Fig. 1. The cell consists of 316 stainless-steel sections screwed together to accept room-temperature hydrogen gas up to 286 atm. An insulated gold-plated copper rod of 0.24 cm diameter runs vertically down the center to a copper disk plated with gold, which constitutes one parallel plate of the cell. The other parallel plate lies below it and is part of the steel cell chassis. This surface is likewise gold plated. The D-T gas enters from below through a 0.075-cm inner-diameter fill tube and passes through a crack between an alumina spacer and the D-T sample space. The lower plate and chassis are electrically separated from the upper plate and copper rod by tight-fitting alumina insulation. A Teflon plug is placed near the top as a high-pressure gas seal.

The parallel-plate region is designed with special care. Because of the radioactivity of the tritium, the entire unit is massively built. This keeps the number of electrical feedthroughs to a minimum and negates the possibility of using guard rings to avoid electrical field fringing effects at the edges.[29] Instead, we buil a coin-shaped space and filled in the outer part with a ring-shaped alumina spacer. The radius of the upper plate is 1.507 cm, the inner radius of the alumina is 0.500 cm, and the gap width is 0.50 cm. Also, the alumina is cut as a single piece around the edge of the upper plate (thickness 0.107 cm) to prevent arcing across this narrow space.

The assembly rests on a Teflon pad in a steel glove box used for tritium contaminent. The cell chassis and the copper rod or disk can each be floated electrically with the glove box as a grounded shield. When used, aluminum foil is placed over the lucite window of the box to complete the shielding. All electrical leads and connectors outside the box are shielded. Outside, a Keithley 230 power supply is used for low potentials and a Hewlett-Packard HP61110A power supply for high potentials. A Keithley 642 electrometer is used to measure the current, which is converted to current density in A/cm^2 by using a plate area of 0.785 cm^2.

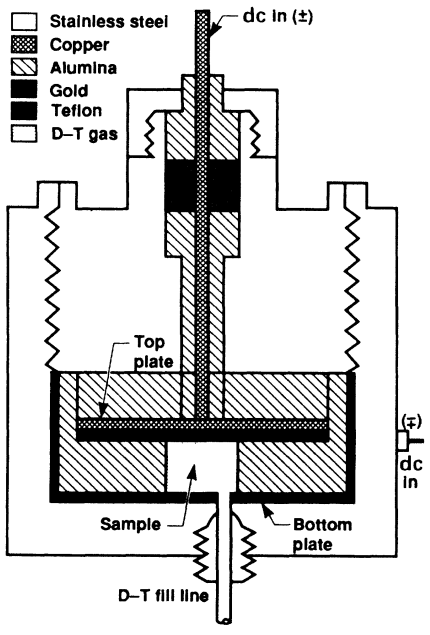

FIG. 1. Schematic of the electrical cell.

An amount of 0.13-mmol T_2 was taken from a palladium bed, passed through a 5-μm stainless-steel frit at 77 K to remove methane, and placed in a stainless-steel bottle at 0.3 atm. Deuterium (initial analysis: 77 ppm N_2, 2.3 ppm O_2, no listed methane) was passed through a 5-Å Linde zeolite bed at 77 K. A quantity of 0.13 mol D_2 was then pumped into the T_2 bottle to 400 atm. By *P-V-T* determinations, the resulting gas was mixed to 0.1 mol % T_2 in D_2 gas, good to ±1%. The T_2-D_2 mix was allowed to stand two days so that the resulting gas contained 0.2% DT and no T_2. At the end of the run, the gas was routinely analyzed by a magnetic sector mass spectrometer and a gas chromatograph. The compositions of the three samples used in this work were T_2, 0.10–0.12 mol %; D_2, 99.33–99.54 mol %; H_2, 0.35–0.57 mol %; N_2 and O_2, 1.3–8.2 molar ppm; methanes, 1.6–4.3 ppm; and Ar, 1.0–1.6 ppm.

The electrical cell was used only for 8-h experiments. Then, it was disassembled, and a new Teflon seal was put in. This was to prevent the buildup of tritium in the Teflon, which could lead to anomalous currents seen in the first trial runs. The alumina parts were soaked in methanol and purged dry with argon passed through a stainless-steel frit. The alumina parts were then baked overnight at 390 K. The cell body was also cleaned in this way. The parts were then reassembled, leak-checked with helium, and pumped out overnight to 10^{-8} torr.

The electrical cell and DT bottle were connected with a Taber-Teledyne 0–350-atm transducer and a uranium bed for the final cleanup. At the start, a zero-pressure current reading was taken. Then the pressure was increased in increments to the values of 2.5, 4.8, 9.7, 24.6, 49.8, 103, 160, 220, and 286 atm. These correspond to the room-temperature gas densities of 0.1, 0.2, 0.4, 1, 2, 4, 6, 8, and 10 mol/l.[30] Each measured current density was taken after a wait of 5 min and represented the steady state. Two measurements were taken at each pressure with reversed polarities. The procedure was repeated in reducing the pressure with a zero-pressure reading being taken at the end. We improved our experiment technique in the first five samples for which the data were discarded. The data was taken on the final three samples. The temperature of measurement was 295±1.5 K.

V. RESULTS AND ANALYSIS

The data are listed in Table I. The empty-cell values have been subtracted from the full-cell data to produce the D-T current densities listed there. The empty-cell current densities are small in every case. The errors of measurement are best shown by the standard deviations listed in Table II. The precision was the worst for the lowest potential of 0.1 V and for the empty-cell blank with the lowest current density. It is possible that a faint

TABLE I. Summary of experimental data for 0.1-mol % T in D_2 gas at room temperature. Three D-T samples—measured with increasing and decreasing pressure—have been averaged. The empty-cell (0-mol/l) values, given in the first row, have been subtracted from the raw data to produce the D-T current densities listed.

Gas density (mol/l)	Average current density in (nA/cm^2) at these dc potentials 0.1 V	1 V	10 V	100 V	400 V
0	1.91×10^{-5}	6.20×10^{-5}	3.79×10^{-4}	3.16×10^{-3}	0.0535
0.1	0.100	0.426	1.41	1.89	2.26
0.2	0.139	0.663	2.20	4.21	4.84
0.4	0.177	0.946	3.16	8.57	9.41
1	0.246	1.401	5.02	16.3	23.1
2	0.193	1.371	5.71	20.5	37.8
4	0.0843	0.751	4.13	17.2	38.1
6	0.0480	0.461	2.83	12.9	30.4
8	0.0331	0.314	2.08	10.2	24.6
10	0.0235	0.226	1.61	8.25	20.5

onset of electron avalanching occurred in the 400-V runs.

The measured current densities as a function of the gas density are shown in Fig. 2 for the different applied voltages. The data are represented by the symbols, whereas the solid lines are the theoretical predictions obtained in the following manner. Repeated calculations were performed keeping all parameters fixed at the values provided in Sec. III except for the two recombination coefficients α_2 and α_3. They were varied in accordance with the expected ranges discussed in Sec. III. For each set of values chosen for α_2 and α_3, the mean-square deviation between predicted and measured result was computed. A contour plot depicted in Fig. 3 shows this deviation. The best agreement between theory and experiment is obtained for combinations of values of α_2 and α_3 in the "valley" that has two branches. The upper branch is, however, at a value of $\alpha_2=2\times10^{-4}$ cm^{-3}s^{-1}, which is at least an order of magnitude above what can be justified theoretically. Therefore, only the lower branch of the valley offers reasonable values for the recombination coefficients. The best fit is achieved with $\alpha_3=6.2\times10^{-26}$ cm^{6}s^{-1} and any value for α_2 below 10^{-5} cm^{2}s^{-1}. These values are very much in line with expectations, and the insignificance of the two-body recombination process in the present experiment is a strong indication that the molecular ions are indeed thermalized prior to recombination.

TABLE II. Standard deviations of the data of Table I. They are shown as percents of the average values listed in Table I.

Gas density (mol/l)	Standard deviation (%) at these dc potentials 0.1 V	1–100 V	400 V
0.0	119	55	161
0.1	56	23	37
0.2	49	21	19
0.4	37	15	9
1.0	20	11	6
2.0–10.0	12	5	9

With the negligible recombination, the cumulative source function $Q(x)$ defined in Eq. (8) becomes proportional to the gas density N. As seen from Eq. (7), the current density is then also proportional to N. Furthermore, as will be seen below, the fraction of the gap from which charges are swept out increases with applied voltage until complete sweep-out is achieved, and for the same voltage this fraction decreases with the gas density or the gap width. Therefore, a relevant parameter is the ratio V/NL or V/N when L is fixed as in the present experiment. Indeed, when I/N is plotted as a function of V/N, all current-voltage curves coincide for gas densities of 2 mol/l or less, as seen in Fig. 4. For higher gas densities, the normalized current-voltage curves remain identi-

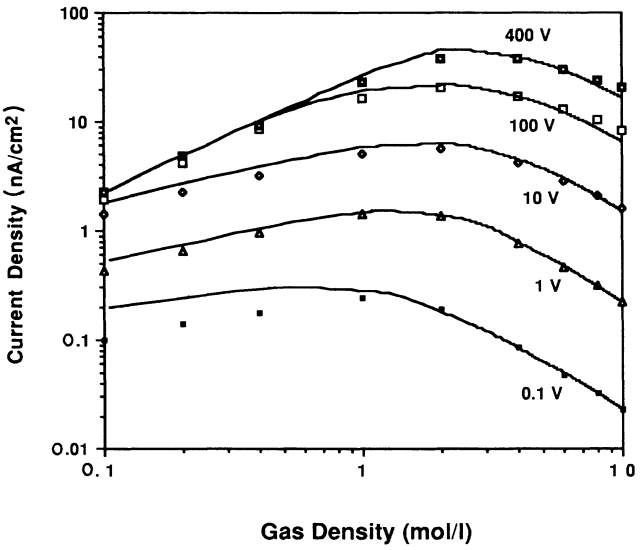

FIG. 2. Measured current densities (data points are the symbols) in D_2 gas with 0.1% tritium and theoretical predictions (solid lines) with properly chosen recombination coefficients.

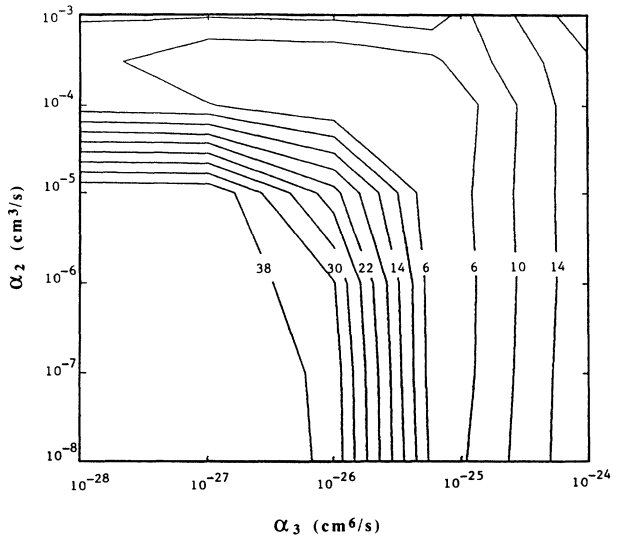

FIG. 3. Mean-square deviation between measured and predicted current densities for varying recombination coefficients.

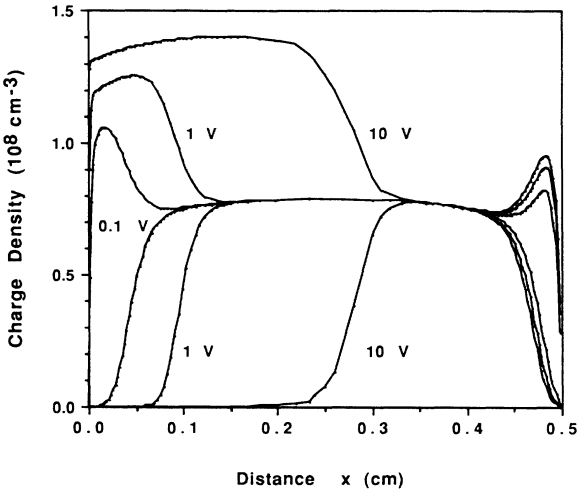

FIG. 5. The charge-density profile for a gas density of 5 mol/l and for the applied voltages indicated. The upper curves are the ion concentrations, and the lower ones represent the electron densities. With the increase in applied voltage, the sweep-out region expands from the cathode side. The charge density is in units of 10^8 cm^{-3}.

cal in shape but are shifted to lower values of I/N because of increase in recombination. Experimental limitations did not allow measurements at very high values of V/N when the gas density was higher than 2 mol/l. However, at sufficiently high voltages, complete sweep-out occurs and the maximum current density I_{max} becomes again proportional to N. As a result, all curves in Fig. 4 converge at high values of V/N to a common plateau of $I_{max}/N = G_0 L/N = 28.4$ nA/cm^2/mol/l. This calculated maximum value indicated in Fig. 3 is seen to be in excellent agreement with the experimentally observed approach to saturation. We emphasize that this agreement is achieved without adjustment of any parameters.

Although the results shown in Fig. 4 indicate that the current is proportional to the applied voltage at low values and becomes less than proportional at higher values, we find no clear regions where a linear and a $V^{1/2}$ relation can be discerned as suggested by the historic work of Thompson.[1,2] Instead, there is a continuous

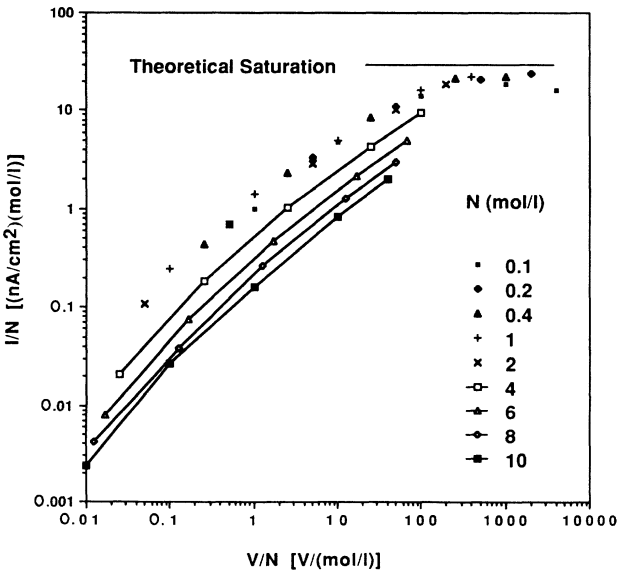

FIG. 4. Measured current densities vs voltage normalized to a gas density of 1 mol/l.

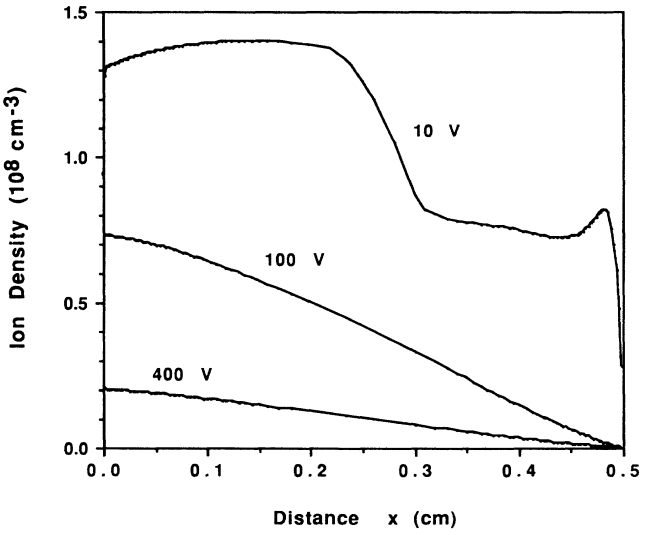

FIG. 6. Ion-density profiles for the same case as in Fig. 5 but at the higher voltages indicated. Complete sweep-out is achieved at and above 100 V, and the electron densities are too low to be shown for 100 and 400 V. The ion density is in units of 10^8 cm^{-3}.

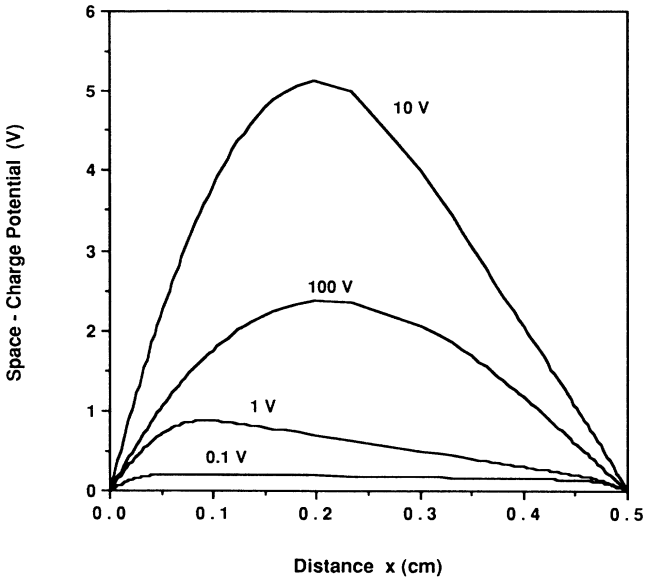

FIG. 7. The space-charge potential throughout the gas gap for the case of a gas density of 5 mol/l and for the applied voltages indicated. The space-charge potential for 400 V is not shown for the sake of clarity. Its profile is equal to the one for 100 V when reduced by a factor of 4.

transition from linear increase to saturation, as is to be expected from the experimental functions contained in our formula (7). In spite of the lack of any distinct features in the current-voltage characteristic, the charge-density profiles exhibit dramatic changes as the applied voltage is increased. This is shown in Figs. 5 and 6 for the case of a gas density of $N=5$ mol/l. With increase in applied voltage, a sweep-out region expands from the cathode side and the recombination region diminishes, as seen in Fig. 5. As long as there remains a recombination region, however, the ion concentration in the sweep-out regions is in fact higher than in the recombination region. After complete sweep-out has been achieved, the ion density profile changes completely, as shown in Fig. 6.

The space-charge potential $\Phi(x)$ (being the total potential minus the applied one) shown in Fig. 7 increases at first as the charge imbalance within the gap becomes more severe. After sweep-out, however, the ions in the gap are extracted faster with increasing voltage, giving a shorter transit time, and hence, a lower ion concentration. As a result, the space-charge potential diminishes again at high values of the applied voltage.

VI. CONCLUSIONS

We have demonstrated in the present paper that small additions of tritium provide a unique method of producing weakly ionized gases at very high densities. Since the ionization is uniform througout the gas, except very close to the walls, an accurate evaluation is possible of the space-charge distributions and of the charge currents under externally applied electric fields. The charge-density profiles within the weakly ionized gas exhibit a complicated structure which changes dramatically as the external voltage is increased. The experimentally measured current-voltage characteristic of a deuterium gas with 0.1% tritium can be brought into close agreement with theoretical results by proper adjustment of the electron-ion recombination rate. In fact, this comparison provides a means to determine electronic recombination coefficients. However, this determination is not unique unless one particular recombination process dominates. For the present experiments, the two-body dissociative recombination process was found to have little influence on the fit of the experimental to theoretical results. As a result, the three-body recombination coefficient could be determined and was found to be

$$\alpha_3=(6.2\pm1.0)\times10^{-26}\ \mathrm{cm}^6\mathrm{s}^{1-}\ \text{at } 298\ \mathrm{K}\ .$$

ACKNOWLEDGMENTS

We would like to thank Raul Garza for the mass spectroscopy of these samples. We are grateful to Chris Gatrousis and Tom Sugihara for funding the experimental work under the Lawrence Livermore National Laboratory Chemistry Research Resource. This work was performed under the auspices of the U. S. Department of Energy by the Lawrence Livermore National Laboratory under Contract No. W-7405-ENG-48 and by Sandia National Laboratories at Livermore under Contract No. DE-AC04-76DP00789.

[1]J. J. Thompson, Philos. Mag. **47**, 257 (1989).
[2]J. J. Thompson and G. P. Thompson, *Conduction of Electricity through Gases* (Dover, New York, 1969), Vol. I, p. 193.
[3]P. E. Boucher, Phys. Rev. **31**, 833 (1928).
[4]W. P. Allis and D. J. Rose, Phys. Rev. **93**, 84 (1954).
[5]M. A. Gusinov and R. A. Gerber, Phys. Rev. A **5**, 1802 (1972).
[6]I. M. Cohen and M. D. Kruskal, Phys. Fluids **8**, 920 (1965).
[7]M. Kurata, *Numerical Analysis for Semiconductor Devices* (Lexington Books, Lexington, MA, 1982).
[8]P. C. Souers, *Hydrogen Properties for Fusion Energy* (University of California Press, Berkeley, CA, 1986), Chap. 16.
[9]D. Combacher, Radiat. Res. **84**, 189 (1980).
[10]L. M. Dorfman, Phys. Rev. **95**, 39 (1954).
[11]A. I. McIntosh, Aust. J. Phys. **19**, 805 (1966).
[12]G. L. Braglia and V. Dallacasa, Phys. Rev. A **18**, 711 (1978).
[13]T. M. Miller, J. T. Mosley, D. W. Martin, and E. W. McDaniel, Phys. Rev. **173**, 115 (1958).
[14]K. Hiraoka and P. Kebarle, J. Chem. Phys. **65**, 746 (1975).
[15]M. T. Elford, J. Chem. Phys. **79**, 5951 (1983).
[16]I. A. Fleming, R. J. Tunnicliffe, and J. A. Rees, J. Phys. B **2**, 780 (1969).
[17]D. R. Bates, J. Phys. B **13**, 2587 (1980); **14**, 3525 (1981).
[18]M. T. Leu, M. A. Biondi, and R. Johnson, Phys. Rev. A **8**, 413 (1973).
[19]B. Pert and K. T. Dolder, J. Phys. B **7**, 1948 (1974).
[20]D. Auerbach, R. Cacak, R. Caudano, T. D. Gailey, C. J.

Keyser, J. W. McGowan, J. B. A. Mitchell, and S. F. J. Wilk, J. Phys. B **10**, 3797 (1977).
[21]J. W. McGowan, P. M. Mul, V. S. D'Angelo, J. B. A. Mitchell, P. Defrance, and H. R. Froelich, Phys. Rev. Lett. **42**, 373 (1979).
[22]J. B. A. Mitchell, C. T. Ng, L. Forand, R. Janssen, and J. W. McGowan, J. Phys. B **17**, L909 (1984).
[23]H. Hus, F. Youssif, A. Sen, and J. B. A. Mitchell, Phys. Rev. A **38**, 658 (1988).
[24]D. Mathur, S. U. Khan, and J. B. Hasted, J. Phys. B **11**, 3615 (1978).
[25]D. Smith and N. G. Adams, Astrophys. J. **284**, L13 (1984).
[26]N. G. Adams, D. Smith, and E. Alge, J. Chem. Phys. **81**, 1778 (1984).
[27]D. Mathur, L. B. Halsted, and S. U. Khan, J. Phys. B **12**, 2043 (1979).
[28]D. R. Bates, V. Malaviya, and N. A. Young, Proc. R. Soc. London Ser. A **320**, 437 (1971).
[29]*Methods of Experimental Physics: Classical Methods,* edited by I. Eastmann (Academic, New York, 1959), pp. 495–496.
[30]Reference 8, p. 135.

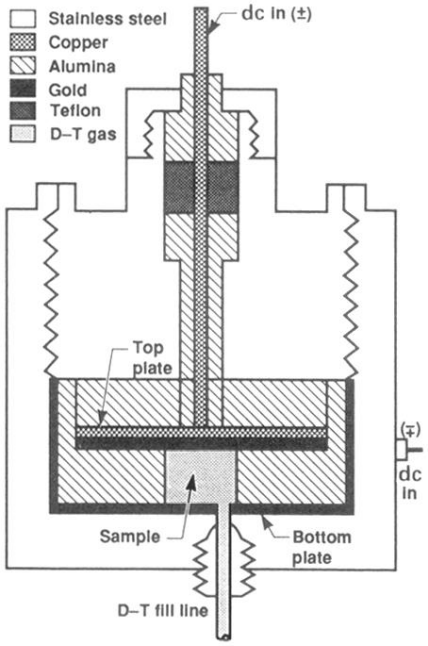

FIG. 1. Schematic of the electrical cell.